Biointerface Research in Applied Chemistry
Open-Access Journal (ISSN: 2069-5837)

Article
Volume 14, Issue 5, 2024, 113
https://doi.org/10.33263/BRIAC145.113

Effect of Addition of Various Amounts of Kaolin Clay on the Properties of a Terpolymer of Vinyl Acetate (VAc), Butyl Acrylate (BA), and Acrylic Acid (AA)

Maromi Roy [1], Uddhab Kalita [2], Nabendu B. Pramanik [3], Madhabi Bhattacharjee [4], Jayanta Barman [5], Dhruba J. Haloi [6,*]

1 Bodoland University, Kokrajhar, Assam-783370, India
2 Indian Institute of Technology Kharagpur, West Bengal-721302, India
3 Institute of Chemical Technology Mumbai –IOC Odisha Campus, Bhubaneswar-751013, India
4 Bodoland University, Kokrajhar, Assam-783370, India
5 A.D.P College, Nagaon, Assam, India
6 Tezpur University, Tezpur, Assam-783370, India
* Correspondence: dhruba2k3@gmail.com;

Scopus Author ID 35275016000
Received: 15.11.2023; Accepted: 28.01.2024; Published: 21.07.2024

Abstract: This study describes preparing and characterizing poly(vinyl acetate) (PVAc) based terpolymer/kaolin clay composites. Conventional free-radical emulsion polymerization was used to prepare a terpolymer of vinyl acetate (VAc), butyl acrylate (BA), and acrylic acid (AA). ^{1}H NMR analysis confirmed the successful preparation of the terpolymer. The conversion of the monomers was calculated gravimetrically and found to be 90 % after one hour of polymerization time. Different amounts of kaolin clay were added to the terpolymer latex and were mixed to prepare the terpolymer/kaolin clay composites. NMR, FT-IR, TGA, DSC, and FESEM analyses were used to characterize the terpolymer and terpolymer/clay composites. Mechanical properties such as tensile strength, modulus, and elongation at the break of the prepared terpolymer/clay composites were also evaluated. A rubber process analyzer (RPA) was used to study the rheological properties of the polymer composites. All the analyses establish the presence of strong clay-polymer interaction in the composite for which the prepared composites exhibit improved thermal properties.

Keywords: vinyl acetate; emulsion polymerization; clay composite.

1. Introduction

In recent years, the research on synthesizing inorganic-organic polymer hybrid materials such as layer silicate/polymer nanocomposites has attracted great interest due to their wide superior physical, mechanical, and thermal properties compared to the other composites [1-3]. The development of emulsion polymers combined with free radical polymerization (FRP), which usually involves two or more monomers in polymerization, has always been of great industrial importance because of its simple preparation methods and wide range of applications [4]. The FRP method is used to produce millions of tons of polymers worldwide [5]. This is due to the wide variety of functional groups well-suited to free radicals [6]. Terpolymers, which are made up of three different monomers that are polymerized together to form a single polymer, have several advantages[7] and applications[7-9] over other polymers as different properties can be combined into a single polymer if the monomers are chosen

carefully [7]. Many studies have been published on producing and characterizing various terpolymers and their films with multiple properties for various applications [7,10,11]. Urrtabizkaia *et al.* investigated the use of VAc, methyl methacrylate (MMA), and BA monomers to synthesize emulsion polymerization. Their kinetics, terpolymer composition, and the total number of polymer particles were also evaluated [7]. Unzue *et al.* used different polymerizable surfactants to perform semicontinuous emulsion polymerization of poly(styrene-co-BA-co-AA). The emulsion polymer latices' particle size, surface tension, and stability against electrolyte solutions were reported [12]. Carter *et al.* investigated VAc, 2-Methylene-1, and 3-Dioxepane emulsion polymers with various properties of novel classes of recyclable, upcyclable, or biodegradable polymers [13]. Elmahdy *et al.* synthesize poly(vinyl chloride-co-vinyl acetate-co-2-hydroxypropyl acrylate) terpolymer and study the enhancement of specific capacitance containing tetrabutylammonium tetrafluoroborate ionic liquid [14]. Nanofibers are produced from copolymers and terpolymers of vinyl phosphonic acid, acrylonitrile, methyl acrylate, and vinyl acetate [15]. Shabnam *et al.* investigated the effect of the third monomer on the polymerization of lauryl methacrylate and MMA in emulsions. They discovered that the nature of the third monomer strongly influences the polymerization rate, polymer properties, and latex properties [16].

A composite is a microscopic blend of two or more polymeric, metallic, or ceramic materials that are linked together in specific ways [17]. Clay composites (organic/inorganic hybrid materials) are made up of clay intercalated with a liquid polymer, with the intercalation group consisting of aluminosilicates of the smectite group [18]. Clays are naturally occurring, readily available silicate minerals. This has led to their widespread use in novel chemical processes, owing to the material's low cost and environmentally friendly nature. Few studies have described how different clays, such as montmorillonite, mica, hectorite, bentonite, or laponite, can be used to stabilize emulsion colloidal latex using the emulsion polymerization technique and clay minerals colloidal latex [19,20]. Sheeted of stable aqua silicates of aluminum, iron, and magnesium, sheeted tape, and mixed-sheeted structures are found in the structure of the clays. Due to this structural feature, clay has a high dispersity, hydrophilicity, sorption ability, ion exchangeability, and the highest tendency to adsorb various organic compounds [21]. Kaolin is a clay mineral commonly used for filling and paper coating [22]. With the chemical formula $Al_2Si_2O_5(OH)_4$, it is a one-of-a-kind phyllosilicate mineral. One tetrahedral SiO_4 silica is linked through an oxygen atom to one octahedral $Al_2(OH)_4$ alumina plate in the 1:1 di-octahedral structure of kaolin clay [23]. Kaolin improves paper appearance and printability by improving properties such as gloss, smoothness, brightness, and opacity [24]. The use of a suitable coupling agent to modify kaolinite can result in good filler particle compatibility and dispersibility in a specific polymer matrix [25].

Despite the fact that the chemistry of polymer intercalation with clay has been known for a long time, the research field of polymer/clay nanocomposites has gained momentum only after the report on the Nylon-6/clay nanocomposites by the Toyota research group [26,27]. Several polymer/clay nanocomposites have recently been created using various monomers [28]. Polymer/clay nanocomposites combine the benefits of organic materials, such as flexibility and moldability, with the strength and heat stability of inorganic materials [29]. Clay particles play a leading role in the polymer stabilizer [30]. These changes are usually the result of the important role of silicate layers (on the dimension and the degree of dispersion). Clay dispersion in the polymer matrix inhibits polymer chain movement, resulting in a significant reinforcing effect [31].

The intercalation of polyvinyl acetate (PVAc) with clay improved the composite properties and has some interesting applications. Compared to pure polyvinyl acetate, Mohsen-Nia *et al*. found that PVAc/montmorillonite nanocomposites have a higher glass transition temperature and thermal stability [32]. Mrah *et al*. investigated polymer/Maghnite nanocomposites that improve thermal stability and mechanical and electrical (electrical conductivity increases) properties, which are useful in materials in flexible electronics and conductive coatings [33]. Rubber/poly (ethylene-co-vinyl acetate) nanocomposite materials have maximum mechanical properties and the lowermost loss factor, which is applied as reuse of tires in the rubber industry [34]. Recently, quantum dots/ethylene VAc copolymer composite films for lighting applications and flexible displays were reported by Li *et al*. [35]. Poly(ethylene-co-VAc) composites with silver-calcined scallop shell powder have good antibacterial properties and could be used in food packaging and biomedical sample storage [36]. Vinyl acetate is a superiorly green monomer, and their copolymers prepared using various methods have a variety of applications [37-40], indicating the potential eco-friendliness of this study of a novel type of terpolymer composites [41]. The Kaolin clay was chosen because of its non-toxicity, ease of availability, and affordability. It may be used to enhance filler particle compatibility and dispersibility in a particular polymer, improve its biodegradation nature, and enhance the barrier properties. Kaolin enhances the barrier properties of water vapor. Kaolin increases the biodegradation nature of polymer/clay composites. That makes polymer/clay composites more suitable as film [42]. This study uses emulsion polymerization to synthesize terpolymer, a simple and environmentally friendly experiment [41].

In recent times, an effort has been made to progress on the preparation of tailor-made polymer-clay composites that illustrate the random distribution of the single-layered silicate and offer additional control over the polymer design [43]. If the monomers are chosen carefully, then terpolymers of vinyl acetate overcome some disadvantages of homopolymer, which makes it unique. As a result of the prospectus of various applications and the green aspect of using vinyl acetate monomer, future research in this field is of great interest.

In this study, we used emulsion polymerization to make poly(VAc-co-BA-co-AA) terpolymers, and five batches of polymer/clay composites were made using different clay loadings. To the best of our knowledge, this is the first account in the study of the effect of kaolin clay on poly(VAc-co-BA-co-AA) terpolymers. The composites were characterized using various analytical techniques such as ^{1}H NMR, FT-IR, DSC, TGA, and SEM. Tensile testing was used to evaluate the mechanical properties of the terpolymer composites. RPA was employed to investigate the rheological behavior of the polymer/clay composites. The synthesis terpolymer/clay composites show better modulus or reinforcement properties than other copolymer/clay composites.

2. Materials and Methods

2.1. Materials.

Vinyl acetate (VAc) (99%, SRL, India), Butyl acrylate (BA) (99%, Aldrich, USA), and Acrylic Acid (AA) (99%, Loba, India) were used after the removal of stabilizing agents present. Potassium persulfate (KPS) (98%, Avra Synthesis Pvt., India), Sodium dodecyl sulfate (SDS) (99%, SRL, India), and Kaolin Clay (Oxford Lab fine Chem LLP) were used as received. Distilled water was used for all the experiments.

2.2. Synthesis of poly(vinyl acetate-co-butyl acrylate-co-acrylic acid).

In a typical terpolymerization reaction, distilled water (164 g, 9.11 mol) and the surfactant SDS (3.28 g, 11.37 mol) were combined in a dry round bottom flask (RB) with a stirrer, magnetic bar, and rubber septum. After 15 minutes of stirring, different compositions of VAc/BA/AA monomers (total 82 g) were injected into the RB. After another 30 minutes of stirring, initiator KPS (0.656 g, 2.42 mmol) was added to the reaction mixture and stirred for an hour. After that, the RB was sealed, and nitrogen gas was passed through the mixture for 60 minutes to remove any dissolved oxygen. Then, the reaction RB was placed in a preheated oil bath with a reflux condenser, and the polymerization reaction was allowed to run for 60 minutes at 470 rpm at 70°C. The conversion was determined gravimetrically after the aliquot was removed at the end of the polymerization.

2.3. Preparation of terpolymer/kaolin clay film.

The prepared terpolymer latex was stirred at 540 rpm for 24 hours at room temperature to obtain a uniform latex. Filtering the solution separates the coagulum from the solution, and the coagulum percentage was calculated to be 3.2 percent. The stable latex was mixed with kaolin clay in various ratios of 5%, 10%, 15%, and 20%, respectively concerning latex. After 36 hours of stirring at 540 rpm, the latex mixtures were transferred to a glass petri dish. The latex mixtures were dried for two days at 60°C in an oven to make a uniform film. NMR, FTIR, DSC, and TGA analyses were performed on the obtained films (terpolymer/clay composites). The prepared terpolymer/clay composites were also evaluated for mechanical properties such as tensile strength, modulus, elongation at break, and hysteresis. The RPA was used to assess the rheological properties of the polymer composites.

2.4. Characterization.

On a 600 MHz Bruker NMR spectrometer, ^{1}H NMR spectra of the terpolymer and the terpolymer/clay composites were recorded using chloroform-d ($CDCl_3$) as a solvent and tetramethylsilane (TMS) as an internal standard. Bruker Topspin 3.6.1 software was used to evaluate the spectra.

With a PerkinElmer (Model spectrum-2) FTIR spectrometer, FTIR spectra of terpolymer and terpolymer/clay composites were recorded for a range of 400 to 4000 cm^{-1} in ATR mode.

The glass transition temperatures (T_g) of the terpolymer and terpolymer/clay composites were determined using a TA DSC25 instrument at a heating rate of 10°C/min from –80°C to 200°C measurements. TGA of the terpolymer/clay composites was performed in the Shimadzu TGA-50 instrument. Under a nitrogen atmosphere, a small sample (approximately 15 mg) was heated from room temperature to 700°C at a heating rate of 10°C/min.

Tensile tests were carried out in a Zwick/Roell Universal testing machine (UTM) with a load cell of 500N and a cross-head speed of 200 mm/min, according to ASTM D412 standards. The polymers were cast over a Teflon Petri dish, dried in a vacuum, and then cut into dumbbell-shaped specimens (thickness 0.85-2.52mm) with the proper dimensions (width 3-3.15 mm). The test was performed on three specimens from the same sample, and the average of all results is shown here. Mechanical properties of terpolymer/clay composites were measured, including tensile strength, modulus, and elongation at break. Hysteresis tests of terpolymer/clay composites were also performed with a Zwick/Roell UTM at 100 percent

maximum strain, 200 mm/min cross-head speed, 500 N load, and 4 strain cycles. The samples were prepared in the same way as the tensile tests.

RPA 200000 equipped with biconical dies was used to evaluate rheological properties, such as the dynamic melt rheological behavior of the terpolymer/clay composites. The specimens were thoroughly loaded between the dies, which were kept at 100°C, and the test was performed in both strain and frequency sweep modes. To establish the linear viscoelastic (LVE) region, the strain sweep mode was used from 7 to 200 percent at a constant frequency of 0.50 Hz, and the frequency sweep mode was used to vary the frequency range from 0.7 to 200 Hz at a constant strain amplitude of 7 percent. To ensure that the rheological nature was in the linear viscoelastic region, a strain of 7% was chosen. The rheological properties of the composites were measured, including storage modulus (G′), loss modulus (G″), loss factor (tanδ) on strain amplitude at a constant frequency, and complex modulus (G*), storage viscosity (η') and complex viscosity (η*) on the frequency at constant strain amplitude.

The morphology of the polymer composites was evaluated using a Field Emission Scanning Electron Microscope (FESEM) (JEOL) micrograph with an accelerating voltage of 5.0 kV.

3. Results and Discussion

The poly(VAc-*co*-BA-*co*-AA) terpolymer (Scheme 1) of VAc, BA, and AA monomers was prepared by FRP using an emulsion polymerization technique. The reaction was carried out at 70°C for 60 minutes at 470 rpm. For the synthesis of terpolymer latex, the KPS initiator was combined with the SDS surfactant in an emulsion polymerization process. The monomer conversion for the polymerization was determined by gravimetric analysis and was found to be 90% after 1 hour. The latex was found to be stable even after a few weeks of storage, as evidenced by UV-visible analysis. The molecular weight of the terpolymer was determined by GPC analysis and was already reported in our earlier research publication [41]. The number average molecular weight for this terpolymer was found to be 100 217 g/mol. Various amounts of kaolin clay were added to this terpolymer latex to prepare the polymer/kaolin clay composites. Table 1 summarizes the compositional breakup of the ingredients involved in making the polymer/kaolin clay composites.

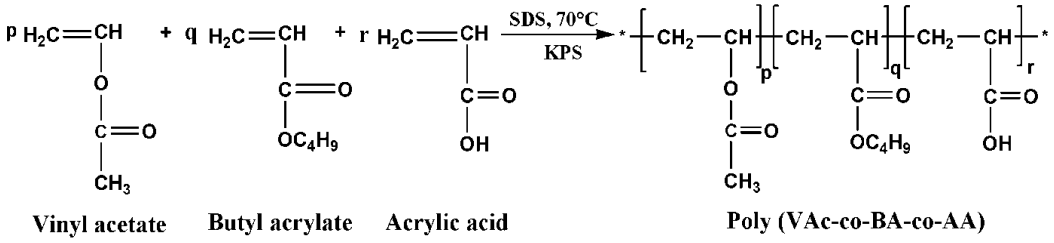

Scheme 1. Terpolymerization of vinyl acetate, butyl acrylate, and acrylic acid.

Table 1. The details of the preparation of the polymer/kaolin clay composites.

Sample Name	Polymerization System	Mole Ratio	Conversion %	Polymer Latex(g)/ Kaolin Clay (g)	% of Kaolin Clay
*V-1				55/0	0
V-2				45/2.25	5
V-3	VAc / BA/AA	0.15/ 0.51/0.14	90	45/4.5	10
V-4				45/6.75	15
V-5				33/6.6	20

* V-1 indicate for poly(VAc-*co*-BA-*co*-AA) and V-2, V-3, V-4, V-5 for poly(VAc-*co*-BA-*co*-AA)/clay composites with 5%, 10%, 15%, 20% respectively.

3.1. Nuclear magnetic resonance spectrometry (^{1}H NMR) analysis.

The 1H NMR spectrum confirmed the incorporation of the monomers. The ^{1}H NMR spectra of poly(VAc-*co*-BA-*co*-AA) and poly(VAc-*co*-BA-*co*-AA)/clay composites are shown in Figures 1 and 2, respectively. In Figure 1, the signal at δ =0.96 (a) and 1.99 (f) ppm are attributed to the BA and VAc methyl protons, respectively. Signals at δ =1.39, 1.62, and 4.06 ppm are assigned to the protons of —CH_2— (b), —CH_2— (c), and —O—CH_2— (d) of BA, respectively. Signals at δ =1.92 and 2.36 ppm correspond to the backbone protons of —CH— (e) and —CH— (g) of BA and AA, respectively. The ^{1}H NMR spectra of poly(VAc-*co*-BA-*co*-AA)/clay composites with different kaolin clay ratios are shown in Figure 2.

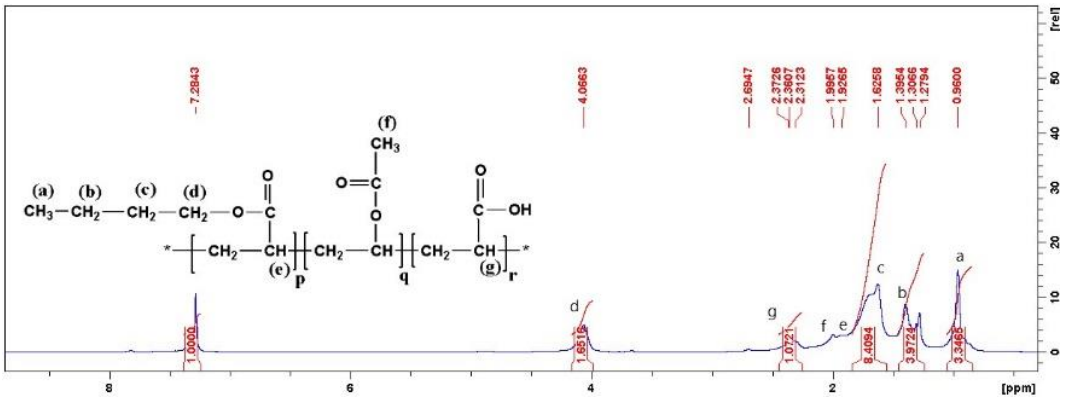

Figure 1. ^{1}H NMR spectrum of poly(VAc-*co*-BA-*co*-AA) terpolymer.

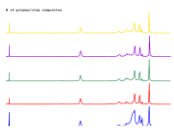

Figure 2. ^{1}H NMR spectra of poly(VAc-*co*-BA-*co*-AA)/clay composites.

3.2. Fourier transform infrared spectroscopy (FTIR) analysis.

The FT-IR spectra for the carbonyl group absorption of terpolymer in the presence of different clay concentrations, t_c, was shown in Figure 3(a). In this spectrum, it was seen that as t_c increases, the absorption band position of >C=O stretching shifts to a lower frequency range (by 1 cm^{-1} in case of 5%, 2 cm^{-1} in case of 10%, 3 cm^{-1} in 15%, and 4 cm^{-1} in 20%). Figure 3(b) shows that with increasing clay amount, Al—O stretching frequencies of kaolin clay shifted to a higher frequency (473.83 cm^{-1} in case of 5% clay, 476.34 cm^{-1} in case of 10% clay, 477.06 cm^{-1} in 15% clay, 478.85 cm^{-1} in 20% clay). It means that when the >Al=O group of the clay layers interacts with the >C=O group of the acrylate monomer (>$C^{\delta-}$=$O^{\delta+}$·····$^{\delta-}$Al=O) (Scheme S1), the double bond nature of the carbonyl group is reduced, and the absorption band

frequency decreases [42]. Figure 3(a) shows C—H stretching of polymer composites at 2961, 2960, 2959, 2958, and 2957 cm^{-1} [18]. In comparison to pure polymer, the C—H stretching band of polymer composites shifted towards a lower frequency (by 1 cm^{-1} in case of 5%, 2 cm^{-1} in case of 10%, 3 cm^{-1} in 15%, and 4 cm^{-1} in 20%). This refers to the adsorption of polymer and kaolin clay particles via hydrogen bonding between the Si—O—H (silanol) of clay and the polymer molecules [43]. Figure 3(b) shows the bands at 1061 and 1070 cm^{-1}, corresponding to Kaolin clay's Si—O stretching frequencies. Similarly, the shift in kaolin's Al—O—Si stretching frequencies was observed at 536, 533 cm^{-1} [44]. The frequency of Si—O groups in kaolin is slightly reduced as a result of polymer molecules interacting with clay particles [43].

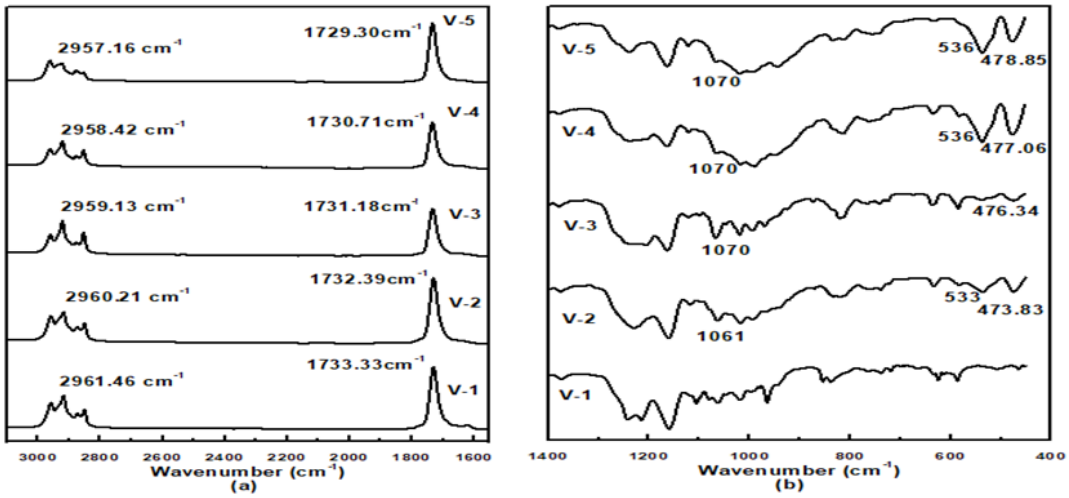

Figure 3. FTIR spectra of terpolymer and terpolymer/clay composites in **(a)** absorption; **(b)** transmittance mode.

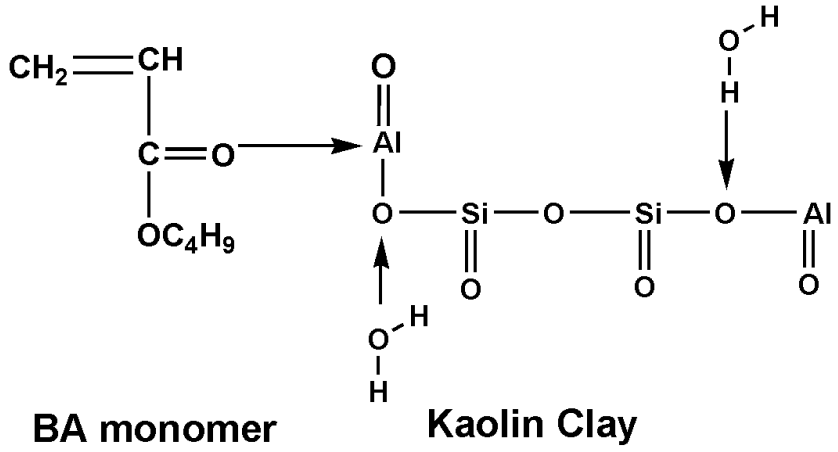

Scheme 2. Schematic presentation of chemical interaction of >C=O groups of BA with -Al=O groups of clay.

3.3. Differential scanning calorimetry (DSC) analysis.

The T_g of the terpolymer/clay composites was determined using DSC measurements. The T_g values of V-1, V-2, V-3, V-4, and V-5 terpolymer/clay composites were found to be –42, –41, –40, –39, and –38°C respectively, as shown in Figure 4, and the same also have been summarized in Table 2. With an increase in the amount of clay, the T_g values shifted toward higher temperatures. The presence of clay in the polymer matrix decreases the free segmental motion of the polymer chains and hence increases the glass transition temperature [2]. The reported *Tg* of polyvinyl acetate/ montmorillonite nanocomposite is 32.2°C to 36.2°C [45,31], which is much higher than the *Tg* of terpolymer/clay composites prepared in this work. Low *Tg* indicates the amorphous nature of the composites.

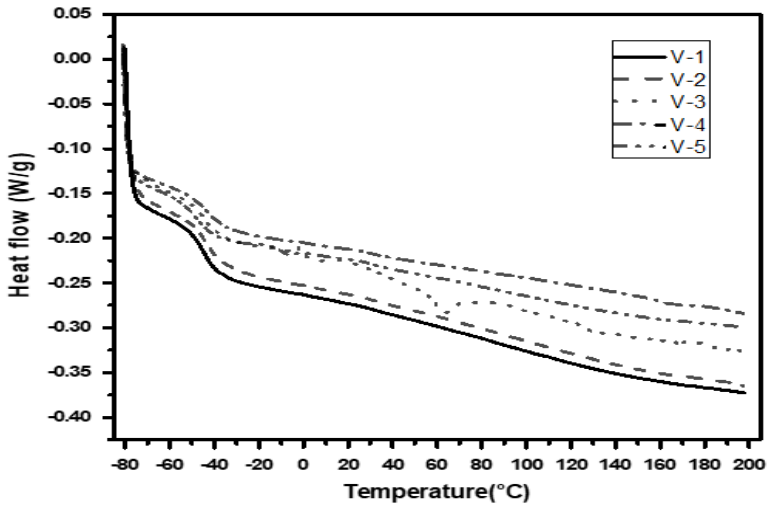

Figure 4. DSC plots of terpolymer and terpolymer/clay composites.

3.5. Thermogravimetric analysis (TGA) analysis.

The thermal stability of the terpolymer/clay composites was investigated using TGA. The different TGA and Derivative thermogravimetry (DTG) curves of terpolymer and terpolymer/clay composites are shown in Figures 5(a) and 5(b). The degradation temperature of terpolymer and terpolymer/clay composites is summarized in Table 2. It shows that terpolymer/clay composites have higher thermal stability than pure terpolymer. The stability of polymer clay composites improves as the amount of clay in the composites increases. This is due to the chemical attachment of the kaolin clay particles to the polymer chains [2]. Batistella *et al.* studied ethylene-VAc/kaolinite composites and observed a two-stage degradation in TGA curves [46], whereas, in this work, a single-stage degradation pattern is observed. The T_{max} values (highest is 540°C) reported in this work are also comparatively higher than the values reported by Batistella *et al.*

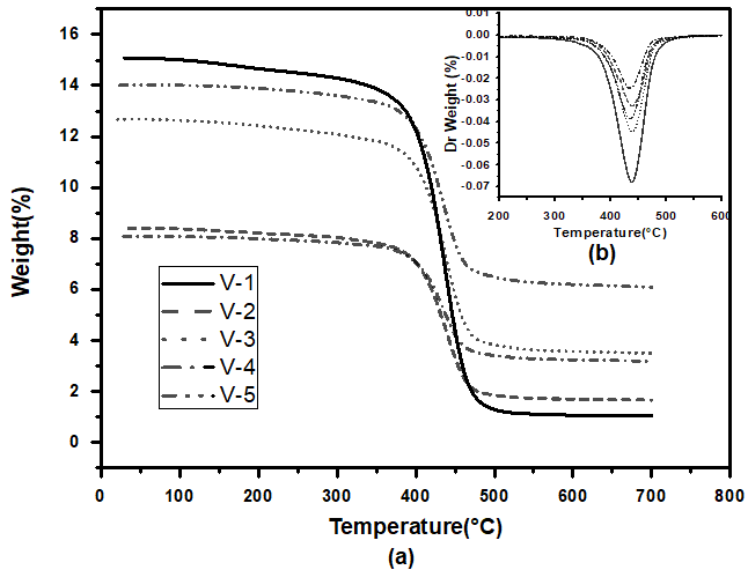

Figure 5. (**a**) TGA; (**b**) DTG plot of terpolymer and terpolymer/clay composites.

Table 2. Thermal properties of terpolymer and terpolymer/clay composites.

Sample	**Kaolin loading (%wt w.r.t. polymer wt)**	**T_{onset} (°C)**	**T_{max} (°C)**	**T_g (°C)**
V-1	Nil	293	508	-42
V-2	5	314	518	-41

Sample	Kaolin loading (%wt w.r.t. polymer wt)	T_{onset} (°C)	T_{max} (°C)	T_g (°C)
V-3	10	329	523	-40
V-4	15	331	527	-39
V-5	20	338	540	-38[2]

3.6. Physico-mechanical properties of terpolymer/clay composites.

Mechanical properties such as tensile strength, modulus, and elongation at the break of the terpolymer have been listed in Table 3. Table 3 shows that in the case of composites, the reinforcement of clay in terms of tensile modulus at 50%, 100%, 200%, and 300% elongation increased with increasing the surface area of the kaolin clay (or increase of the percentage of kaolin clay) in the compositions up to V-4, after which it decreased with further increase of clay loading. The tensile strength of the composites decreased as the amount of kaolin clay in the mixture increased to a very high extent. The composites' strength was reduced due to clay aggregation at very high clay loading [47]. Elongation at break decreased as the percent of kaolin clay (or the surface area of composites) increased up to V-3, after which it decreased (in the composite V-5). This is due to the improved polymer reinforcement and internal plasticizing effect imparted by the clay present in the polymer. In contrast, elongation was reduced due to the aggregation tendency of clay at higher clay loading [48]. The reinforcement parameter refers to the physico-mechanical properties of the materials. As a result, as the amount of clay in the composites increases, the physico-mechanical properties of the polymer increase.

Table 3. Physico-mechanical properties of terpolymer and terpolymer/clay compositions.

Sample name	a_0 (mm)	b_0 (mm)	Modulus at 50% (MPa)	Modulus at 100% (MPa)	Modulus at 200% (MPa)	Modulus at 300% (MPa)	Tensile Strength (MPa)	Elongation at break (%)	Wa (Nm)	F-max (MPa)
V-1	2.52	3.15	0.065	0.098	0.175	0.276	1.290	962.6	1.43	1.290
V-2	2.14	3.00	0.122	0.167	0.258	0.354	0.830	821.8	0.81	0.832
V-3	1.20	3.00	0.139	0.187	0.295	0.378	0.211	508.8	0.19	0.440
V-4	0.85	3.00	0.175	0.187	0.189	0.188	-	-	-	0.193
V-5	1.30	3.00	0.170	0.171	0.166	0.160	0.050	995.1	0.17	0.175[3]

3.7. Hysteresis test.

The hysteresis loss of polymer compounds is compared in Figure 6 with composite films' thickness (1.3 mm- 2.30 mm) and width (3 mm). The hysteresis loss, known as the Mullins effect, is a stress-softening technique. The Mullins effect describes the amount of energy generated when a cyclic deformation occurs. In terms of viscoelastically and hydrodynamically, the hysteresis of polymer composites increases as the amount of clay or the specific surface area of clay increases. The different specific surface area of polymer/clay blends impacts clay minerals [48]. The amount of hysteresis loss area under the curve was calculated using Origin 8 computer software. Meneghetti *et al*. reported that the hysteresis loop created by short glass fiber and polypropylene increased with the number of cycles [49]. Figure 5 shows that cyclic energy loss is lower in the first cycle than in the second cycle and that the fourth cycle has the highest hysteresis energy loss. The hysteresis loss increased with the number of cycles in the loop, indicating that energy losses increased with the number of cycles in the loop. This is clearly due to the low filler–filler or terpolymer-clay interaction that takes place at a higher specific surface area filled polymer compound with the increase in the number of cycles. This indicates that the energy dissipation of the polymer composite with clay was

more effective through the loading and unloading cycles. This could be due to the reason for the destruction and delayed restoration of the interactions among the clay particles and the polymer at different strain amounts during the cycles [50].

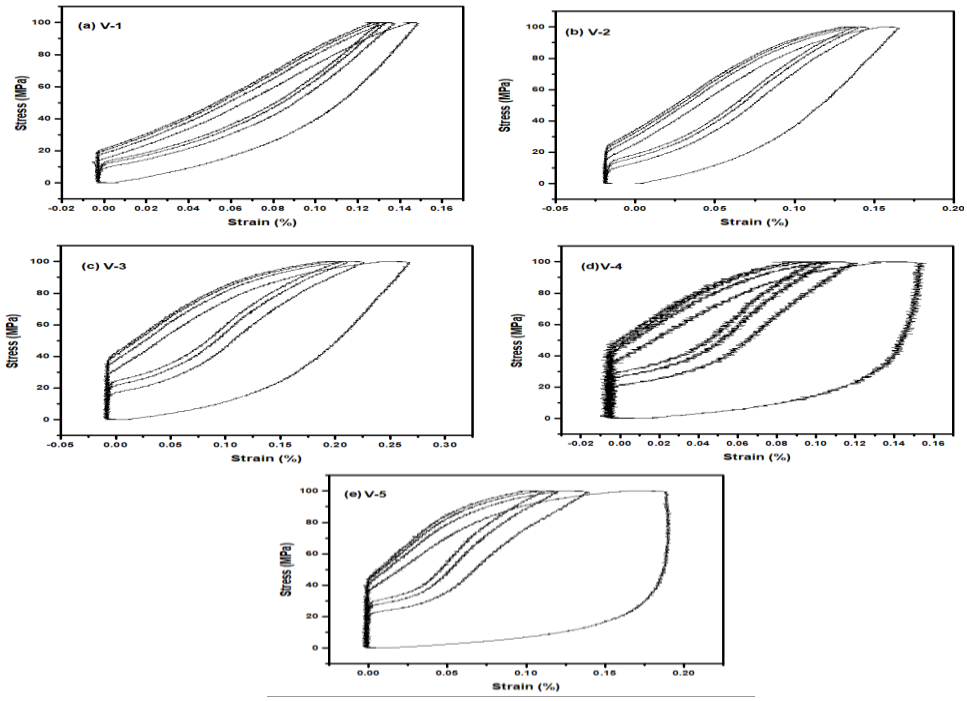

Figure 6. Hysteresis loops for terpolymer and terpolymer/clay composites **(a)** V-1; **(b)** V-2; **(c)** V-3; **(d)** V-4; **(e)** V-5.

3.8. Rheological properties of terpolymer/clay composites analysis.

Using an RPA, the melt rheological properties of the polymer composites were assessed. Dynamic viscoelastic properties of the polymer composites were characterized by storage modulus (G′), loss modulus (G″), and loss factor (tan δ = G″/G′) of the terpolymer and its clay composites under strain sweep and are shown in Figures 7(a), 7(b) and 7(c). Figure 7(a) depicts the terpolymer/clay composites storage modulus (G′) curve, which shows a non-linear viscoelastic behavior, and the modulus decreases with enhancing strain. This demonstrates that there was a structural breakdown. According to Datta *et al.*, in the study of (S–B–S) copolymer of vinyl-styrene, butadiene, and styrene, the modulus decreases with enhancing strain. This is mainly when the temperature rises to 120°C when subjected to increased strain, which causes the uncoiling of polybutadiene units to occur quickly and the fragmentation of polystyrene units into smaller pieces [51]. This is similar to what we found in our research. With increasing strain percent, there is less confrontation in both elastic deformation and viscous flow due to these changes. As a result, the curves showed a sigmoidal decrease in the character [51]. The storage modulus reduction was caused by increasing clay amounts in the composite samples. This may be due to the filler influence of clays and successive interactions with polymer chains in these composites. In fact, the low strain percent of the storage modulus was high for a high clay amount, which features a good dispersion of clay in the polymer matrix. The outcome is useful for estimating the capacity of clay dispersion in the polymer composite matrix. The curve of loss modulus (G″) versus strain percent is shown in Figure 7(b). The loss modulus decreases as the strain percent increases because the materials crack into smaller units. Datta *et al.* also reported that the loss modulus of (S–B–S) copolymer of vinyl styrene, butadiene, and styrene decreased at a certain point with increased strain due to the materials cracking into

slighter units. The approximately same type of findings can be found in our polymer composites [51]. As a result, composites exhibit a flow nature. However, the enhancement of loss modulus in the low-frequency region with an increase in the concentration of clay. This performance and magnitude of modulus development may be due to more interaction of clay and polymer chains because of additional effective dispersion given by clay. Figure 7(c) shows the plot of loss factor (tan δ) versus strain % for terpolymer/clay composites, which shows that as the clay content increased, the strain% and the tan δ also increased. The improved flow behavior (or enhancement of viscous property) in the direction of the shear strain helped by the polymer composites in the molten state may be the reason for the high value of tan δ for more clay amount composites [52]. The loss factor increases with the increase in the clay concentration, mainly due to the interaction of polymer and clay. Concisely, the rheological report indicates that there is a stronger interaction between kaolin clay and terpolymer chains. Frequency sweep experiments were used to investigate the melting behavior of the terpolymer/clay composite samples. The plot of complex modulus (G*) on frequency is shown in Figure 8. Throughout the frequency range, the modulus decreases as the frequency increases.

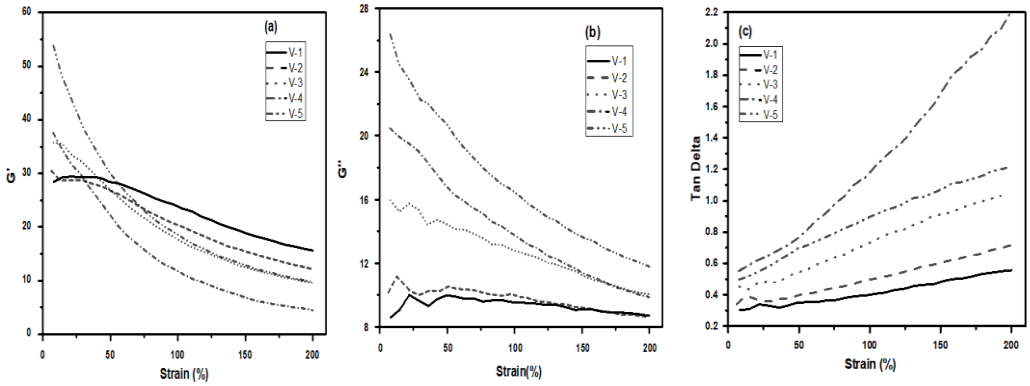

Figure 7. (a) Storage modulus; **(b)** loss modulus; **(c)** loss tangent plots for the terpolymer and its composites.

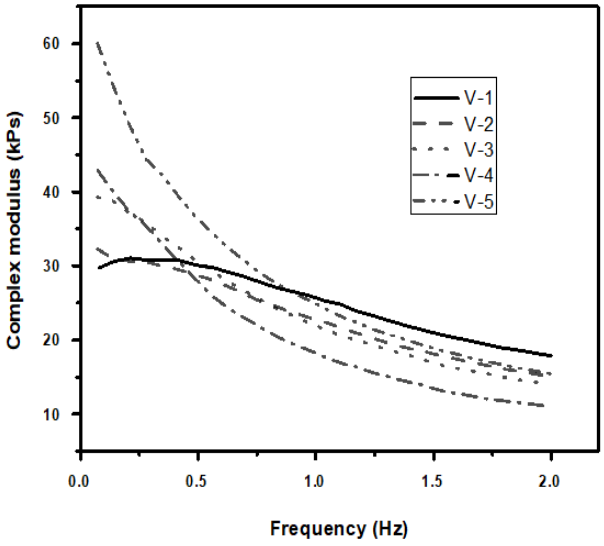

Figure 8. Complex modulus as a function of frequency (Hz) of terpolymer and terpolymer/clay composites.

Figure 9(a) depicts the relationship between storage viscosity (dynamic viscosity) and frequency. The results show that storage viscosity (η') decreases as the frequency of storage increases. According to Datta *et al.*, the real component of the complex viscosity ($\eta^* = \eta' - i\eta''$) is called the storage viscosity for the melt as a fluid in the theory of viscoelasticity. The loss

modulus G″ is represented by (η′= G″/ω), whereas η″ is the imaginary component representing the melt elasticity, and the relation between η″ and the storage modulus G″ is η″ = G′/ ω [51].

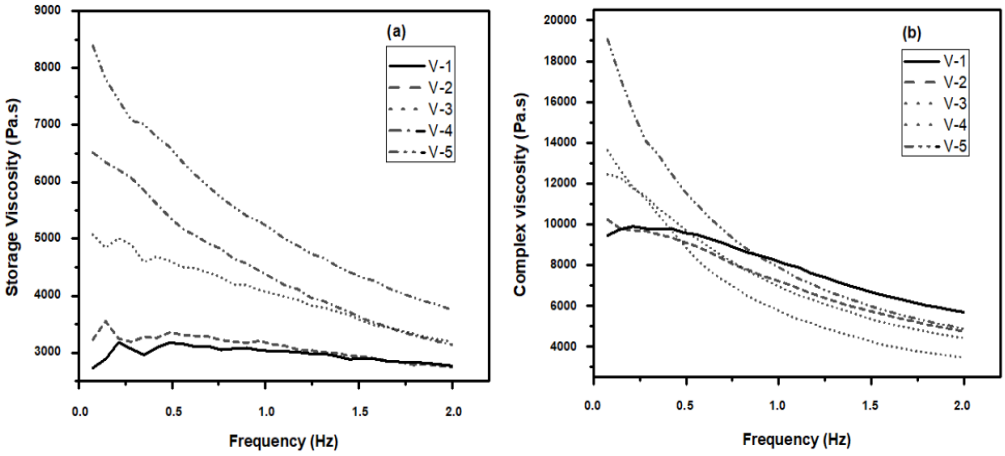

Figure 9. (**a**) Storage viscosity; (**b**) complex viscosity of terpolymer and terpolymer/clay composites.

In frequency sweep mode, the complex modulus of sample V-1 was higher than that of sample terpolymer/Clay composites V-2. It is presented that the incorporation of clay eagerly decreases the modulus from 27.08 kPs for sample V-1 to 24.4 kPs for sample V-2 at a frequency of 83.17 %. In the comparison of the outcomes of the complex modulus for terpolymer and terpolymer/clay composites samples with increasing the clay concentration, indications that terpolymer/clay composites have a more pronounced filler effect using clay of its low molecular weight and, therefore, the low quantity of melt viscosity. This performance and modulus development at the low-frequency region may be due to the higher interaction of clay and polymer chains for more effective clay dispersion [53]. Figure 9(b) shows the plot of complex viscosity as a function of frequency for polymer/clay composites. The results showed that as the shear rate or frequency range increases, all samples' complex viscosity (η*) decreases. This is due to the fact that all polymer composites exhibit pseudoplastic or non-Newtonian fluid behavior. As a result, the polymer composites have good processing characteristics [52]. The storage viscosity increases with an increase in the clay amount. The complex viscosity decreases with the increase in clay amount. These rheological responses indicate a stronger interaction between kaolin clay and terpolymer chains.

3.9. Morphological study.

FESEM was used to examine the surface morphologies of the polymer and the polymer/clay composites. The micrographs for polymer V-1 and polymer/clay V-2 composites are shown in Figure 10.

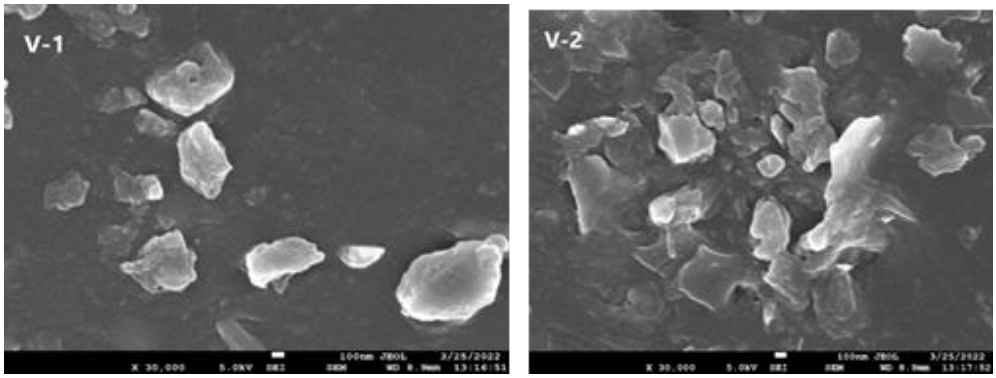

Figure 10. FESEM images of terpolymer (V-1) and terpolymer/clay composite (V-2).

According to these micrographs, polymer composites have a smaller particle size than that of polymer/clay composites. The particle size grows when the clay is added, and agglomeration occurs [54]. This led to a change in the particle size in the terpolymer.

4. Conclusions

Conventional free-radical emulsion polymerization of VAc, BA, and AA yields PVAc-based terpolymer latex. The emulsion polymerization was successfully carried out at 70°C using KPS as an initiator and SDS as a surfactant. The conversion of the monomers after one hour of polymerization was calculated gravimetrically and found to be 90%. The successful incorporation of co-monomers in the terpolymer was confirmed by ^{1}H NMR analysis. A requisite amount of clay is mixed directly with the terpolymer latex to prepare the composites. FT-IR studies reveal a distinct interaction between the >Al=O groups of the clay and that of the carbonyl group in the polymer. The bonding of clay to the polymer chain was confirmed by DSC analysis, where an increase in T_g of the composites was observed with clay loading. According to the TGA and DTG analyses, degradation temperature rises as clay content increases, indicating that clay increases the thermal stability of the composites. As a result, the thermal properties of the composites have improved. The interaction between the polymer and clay was also confirmed via tensile measurements. The tensile strength decreased as the percentage of kaolin composites increased. With the increase of filler loading, the uniform dispersion and adhesion of clay into the polymer matrix increases, which increases the tensile modulus. As a result, clay-based composites improve the physicomechanical properties of polymer films. It was observed that clay's presence enhances the polymer composites' viscous properties in the molten state using an RPA in strain sweep mode. Experiments with frequency sweeps show that the complex viscosity of all composites decreases as the frequency range increases. As a result, polymer composites exhibit pseudoplastic or non-Newtonian fluid behavior. Thus, it can be concluded that the polymer composites have good processing characteristics and may have several potential applications as adhesives.

Funding

This research received no external funding.

Acknowledgments

Declared none.

Conflicts of Interest

The authors declare no conflict of interest.

References

1. Zhang, W.; Chen, D.; Zhao, Q.; Fang, Y. Effects of different kinds of clay and different vinyl acetate content on the morphology and properties of EVA/clay nanocomposites. *Polymer* **2003**, *44*, 7953-7961, https://doi.org/10.1016/j.polymer.2003.10.046.
2. Haloi, D.J.; Ata, S.; Singha, N.K. Synthesis of Poly(2-ethylhexyl acrylate)/Clay Nanocomposite via In Situ and Surface Initiated-Atom Transfer Radical Polymerization. *Adv. Sci. Eng. Med.* **2014**, *6*, 240-245, https://doi.org/10.1166/asem.2014.1432.

3. Cherifi, B.I.; Belbachir, M.; Rahmouni, A.; Derail, C.; Hannaoui, F.; Zeggai, F.Z.; Chebout, R.; Bachari, K. Improvement of the viscoelastic and thermal properties of polyvinyl acetate reinforced with organophilic clay (Algerian MMT). *J. Mol. Struct.* **2023**, *1252*, 132100, https://doi.org/10.1016/j.molstruc.2021.132100.
4. Urretabizkaia, A.; Leiza, J.R.; Asua, J.M. On-line terpolymer composition control in semicontinuous emulsion polymerization. *AIChE J.* **1994**, *40*, 1850-1864, https://doi.org/10.1002/AIC.690401109.
5. Hawker, C.J.; Frechet, J.M.J.; Grubbs, R.B.; Dao, J. Preparation of Hyperbranched and Star Polymers by a "Living", Self-Condensing Free Radical Polymerization. *J. Am. Chem. Soc.* **1995**, *117*, 10763-10764, https://doi.org/10.1021/ja00148a027.
6. Iwasaki, T.; Yoshida, J. Free Radical Polymerization in Microreactors. Significant Improvement in Molecular Weight Distribution Control. *Macromolecules* **2005**, *38*, 1159-1163, https://doi.org/10.1021/ma048369m.
7. Urretabizkaia, A.; Asua, J.M. High solids content emulsion terpolymerization of vinyl acetate, methyl methacrylate, and butyl acrylate. I. Kinetics. *J. Polym. Sci. A. Polym. Chem.* **1994**, *32*, 1761-1778, https://doi.org/10.1002/pola.1994.080320919.
8. Cheng, J.; Shi, X.; Xu, L.; Zhang, P.; Zhu, Z.; Lu, S.; Yan, L. Investigation of the effects of styrene acrylate emulsion and vinyl acetate ethylene copolymer emulsion on the performance and microstructure of mortar. *J. Build. Eng.* **2023**,*75*, 106965, https://doi.org/10.1016/j.jobe.2023.106965.
9. Ramesan, M.T.; Sameela, T.P.; Meera, K.; Bahuleyan, B.K.; Verma, M. In situ emulsion polymerization of poly (vinyl acetate) and asparagus racemosus biopolymer composites for flexible energy storage applications. *Polym. Compos.* **2023**, *44*, 4168-4177, https://doi.org/10.1002/pc.27388.
10. Staicu, T.; Micutz, M.; Leca, M. Electrostatically and electrosterically stabilized latices of acrylic copolymers used as pressure-sensitive adhesives. *Prog. Org. Coat.* **2005**, *53*, 56-62, https://doi.org/10.1016/j.porgcoat.2004.11.010.
11. Gadhave, R.V.; Vineeth, S.K. Synthesis and characterization of starch stabilized polyvinyl acetate-acrylic acid copolymer-based wood adhesive. *Polym. Bull.* **2023**, *80*, 10335–10354, https://doi.org/10.1007/s00289-022-04558-8.
12. Unzué, M.J.; Schoonbrood, H.A.S.; Asua, J.M.; Goñi, A.M.; Sherrington, D.C.; Stähler, K.; Goebel, K.-H.; Tauer, K.; Sjöberg, M.; Holmberg, K. Reactive surfactants in heterophase polymerization. VI. Synthesis and screening of polymerizable surfactants (surfmers) with varying reactivity in high solids styrene– butyl acrylate–acrylic acid emulsion polymerization. *J. Appl. Polym. Sci.* **1997**, *66*, 1803-1820, https://doi.org/10.1002/(SICI)1097-4628(19971128)66:9%3C1803::AID-APP20%3E3.0.CO;2-U.
13. Carter, M.C.D.; Hejl, A.; Janco, M.; DeFelippis, J.; Yang, P.; Gallagher, M.; Liang, Y. Emulsion Polymerization of 2-Methylene-1,3-Dioxepane and Vinyl Acetate: Process Analysis and Characterization. *Macromolecules* **2023**, *56*, 5718–5729, https://doi.org/10.1021/acs.macromol.3c00571.
14. Elmahdy, M.M.; Aldhafeeri, K.A.; Ahmed, M.T.; Azzam, M.A.; Fahmy, T. Molecular dynamics and conduction mechanism of poly(vinyl chloride-co-vinyl acetate-co-2-hydroxypropyl acrylate) terpolymer containing ionic liquid. *Polym. Adv. Tachnol.* **2023**, *34*, 800-816, https://doi.org/10.1002/pat.5932.
15. Keskin, E.; Köken, N,; Kızılcan, N.; Akar, A. Copolymers and terpolymers of vinyl phosphonic acid, acrylonitrile, methyl acrylate, and vinyl acetate. Thermal oxidative stabilization and their nanofiber. *Polym. -Plast. Technol. Mater.* **2023**, *62*, 2030-2042, https://doi.org/10.1080/25740881.2023.2250863.
16. Shabnam, R.; Ali, A.M.I.; Miah, M.A.J.; Tauer, K.; Ahmad, H. Influence of the third monomer on lauryl methacrylate–methyl methacrylate emulsion terpolymerization. *Colloid Polym. Sci.* **2013**, *291*, 2111-2120, https://doi.org/10.1007/s00396-013-2952-7.
17. Majeed, B.A.A.; Sabar, D.A. Effect of Kaolinite on the Mechanical Properties, Thermal Properties, Flammability and Water Absorption Percentage of Poly (Vinyl Chloride) Composite. *Iraqi J. Chem. Pet. Eng.* **2017**, *18*, 27-39, https://doi.org/10.31699/IJCPE.2017.2.3.
18. Gardolinski, J.E.; Carrera, L.C.M.; Cantão, M.P.; Wypych, F. Layered polymer-kaolinite nanocomposites. *J. Mater. Sci.* **2000**, *35*, 3113-3119, https://doi.org/10.1023/A:1004820003253.
19. Kpogbemabou, D.; Lecomte-Nana, G.; Aimable, A.; Bienia, M.; Niknam, V.; Carrion, C. Oil-in-water Pickering emulsions stabilized by phyllosilicates at high solid content. *Colloids Surf. A: Physicochem. Eng. Asp.* **2014**, *463*, 85-92, https://doi.org/10.1016/j.colsurfa.2014.09.037.
20. Guillot, S.; Bergaya, F.; de Azevedo, C.; Warmont, F.; Tranchant, J.-F. Internally structured pickering emulsions stabilized by clay mineral particles. *J. Colloid Interface Sci.* **2009**, *333*, 563-569, https://doi.org/10.1016/j.jcis.2009.01.026.
21. Zhumagaliyeva, S.N.; Iminova, R.S.; Kairalapova, G.Z.; Beysebekov, M.M.; Beysebekov, M.K.; Abilov, Z.A. Composite Polymer-Clay Hydrogels Based on Bentonite Clay and Acrylates: Synthesis,

Characterization and Swelling Capacity. *Eurasian Chem.-Technol. J.* **2017**, *19*, 279-288, https://doi.org/10.18321/ectj672.
22. Bundy, W.M.; Ishley, J.N. Kaolin in paper filling and coating. *Appl. Clay Sci.* **1991**, *5*, 397-420, https://doi.org/10.1016/0169-1317(91)90015-2.
23. Turhan, Y.; Doğan, M.; Alkan, M. Poly(vinyl chloride)/Kaolinite Nanocomposites: Characterization and Thermal and Optical Properties. *Ind. Eng. Chem. Res.* **2010**, *49*, 1503-1513, https://doi.org/10.1021/IE901384X.
24. Zhang, Y.; Liu, Q.; Frost, R.L. Quantitative characterization of kaolinite dispersibility in styrene–butadiene rubber composites by fractal dimension. *Polym. Compos.* **2015**, *36*, 1486-1493, https://doi.org/10.1002/pc.23055.
25. Blumstein, A. Polymerization of adsorbed monolayere. II. Thermal degradation of the inserted polymer. *J. Polym. Sci. A: General Papers* **1965**, *3*, 2665-2672, https://doi.org/10.1002/pol.1965.100030721.
26. Okada, A.; Kawasumi, M.; Usuki, A.; Kojima, Y.; Kurauchi, T.; Kamigaito, O. Nylon 6-Clay Hybrid. *MRS Online Proc. Lib.* **1989**, *171*, 45-50, https://doi.org/10.1557/PROC-171-45.
27. Ogata, N.; Jimenez, G.; Kawai, H.; Ogihara, T. Structure and thermal/mechanical properties of poly(*l*-lactide)-clay blend. *J. Polym. Sci. B: Polym. Phys.* **1997**, *35*, 389-396, https://doi.org/10.1002/(SICI)1099-0488(19970130)35:2%3C389::AID-POLB14%3E3.0.CO;2-E.
28. Moraes, R.P.; Santos, A.M.; Oliveira, P.C.; Souza, F.C.T.; do Amaral, M.; Valera, T.S.; Demarquette, N.R. Poly(styrene-co-butyl acrylate)-Brazilian Montmorillonite Nanocomposites, Synthesis of Hybrid Latexes via Miniemulsion Polymerization. *Macromol. Symp.* **2006**, *245-246*, 106-115, https://doi.org/10.1002/masy.200651314.
29. Moraes, R.P.; Valera, T.S.; Pereira, A.M.C.; Demarquette, N.R.; Santos, A.M. Influence of the type of quaternary ammonium salt used in the organic treatment of montmorillonite on the properties of poly(styrene-*co*-butyl acrylate)/layered silicate nanocomposites prepared by *in situ* miniemulsion polymerization. *J. Appl. Polym. Sci.* **2011**, *119*, 3658-3669, https://doi.org/10.1002/app.33067.
30. Luan, Y.; Ma, X.; Ma, Y.; Liu, X.; Jiang, S.; Zhang, J. Research on strength improvement and stabilization mechanism of organic polymer stabilizer for clay soil of subgrade. *Case Stud. Constr. Mater.* **2023**, *19*, e02397, https://doi.org/10.1016/j.cscm.2023.e02397.
31. Mohsen-Nia, M.; Doulabi, F.S.M. Synthesis and characterization of polyvinyl acetate/montmorillonite nanocomposite by in situ emulsion polymerization technique. *Polym. Bull.* **2011**, *66*, 1255-1265, https://doi.org/10.1007/s00289-010-0399-2.
32. Mrah, L.; Khiati, Z. Influence of Clay on Structure, Thermal Properties and Mechanics of Poly(vinyl acetate)/Maghnite Nanocomposites. *ChemistrySelect* **2023**, *8*, e202301268, https://doi.org/10.1002/slct.202301268.
33. Sadeghi-Askari, A.; Tavakoli, M. Optimization of mechanical and dynamic-mechanical properties of electron beam irradiation of reclaimed tire rubber/poly (ethylene-*co*-vinyl acetate) nanocomposite by design of experiment. *Iran. Polym. J.* **2023**, *32*, 417–431, https://doi.org/10.1007/s13726-022-01135-8.
34. Li, Y.; Lv, Y.; Guo, Z.; Dong, L.; Zheng, J.; Chai, C.; Chen, N.; Lu, Y.; Chen, C. One-Step Preparation of Long-Term Stable and Flexible $CsPbBr_3$ Perovskite Quantum Dots/Ethylene Vinyl Acetate Copolymer Composite Films for White Light-Emitting Diodes. *ACS Appl. Mater. Interfaces* **2018**, *10*, 15888-15894, https://doi.org/10.1021/acsami.8b02857.
35. Manoj, M.; Manaf, O.; Ismayil, K.M.M.; Sujith, A.J. Composites based on poly(ethylene-co-vinyl acetate) and silver-calcined scallop shell powder: Mechanical, thermal, photocatalytic, and antibacterial properties. *J. Elastomers Plast.* **2021**, *53*, 902-921, https://doi.org/10.1177/0095244321996396.
36. Igwe, I.O.; Osuoha, G.; Nwapa, C. Characterization and Utilization of Eziulo Clay as an Extender in Emulsion Paint Formulations. *J. Minerals Mater. Charact. Eng.* **2017**, *5*, 174-184, https://doi.org/10.4236/jmmce.2017.54015.
37. Kwaśniewska, A.; Chocyk, D.; Gładyszewski, G.; Borc, J.; Świetlicki, M.; Gładyszewska, B. The Influence of Kaolin Clay on the Mechanical Properties and Structure of Thermoplastic Starch Films. *Polymer* **2020**, *12*, 73, https://doi.org/10.3390/polym12010073.
38. Liu, J.; Wang, C.; Liu, Q.; Zhang, F.; Liu, X.; Sun, M. Effect of poly(ethylene-vinyl acetate) pour point depressant on the cold flow properties and crystallization behavior of soybean biodiesel blends fuel. *Turkish J. Chem.* **2022**, *46*, 311-319, https://doi.org/10.55730/1300-0527.3308.

39. Farhana, N.K.; Bashir, S.; Ramesh, S.; Ramesh, K. Augmentation of dye-sensitized solar cell photovoltaic conversion efficiency via incorporation of terpolymer Poly(vinyl butyral-co-vinyl alcohol-co-vinyl acetate) based gel polymer electrolytes. *Polymer* **2021**, *223*, 123713, https://doi.org/10.1016/j.polymer.2021.123713.
40. Souto, L.F.C.; Soares, B.G. Electromagnetic wave absorption, EMI shielding effectiveness and electrical properties of ethylene – vinyl Acetate (EVA)/ Polyaniline (PAni) blends prepared by in situ polymerization. *Synth. Met.* **2023**, *298*, 117441, https://doi.org/10.1016/j.synthmet.2023.117441.
41. Roy, M.; Bhattacharjee, M.; Dhar, A.; Baishya, B.; Haloi, D.J. Synthesis and compositional analysis of co- and ter-polymers of butyl acrylate with vinyl acetate and acrylic acid prepared via emulsion polymerization. *Indian J. Chem. Technol.* **2020**, *27*, 509-514.
42. Datta, H.; Singha, N.K.; Bhowmick, A.K. Beneficial Effect of Nanoclay in Atom Transfer Radical Polymerization of Ethyl Acrylate: A One Pot Preparation of Tailor-Made Polymer Nanocomposite. *Macromolecules* **2008**, *41*, 50-57, https://doi.org/10.1021/ma071528s.
43. Duman, O.; Tunç, S.; Çetinkaya, A. Electrokinetic and rheological properties of kaolinite in poly(diallyldimethylammonium chloride), poly(sodium 4-styrene sulfonate) and poly(vinyl alcohol) solutions. *Colloids Surf. A: Physicochem. Eng. Asp.* **2012**, *394*, 23-32, http://dx.doi.org/10.1016/j.colsurfa.2011.11.018.
44. Tironi, A.; Trezza, M.A.; Irassar, E.F.; Scian, A.N. Thermal Treatment of Kaolin: Effect on the Pozzolanic Activity. *Procedia Mater. Sci.* **2012**, *1*, 343-350, https://doi.org/10.1016/j.mspro.2012.06.046.
45. Cazotti, J.C.; Salvato, R.C.P.J.S.; Alves, G.M.; Moreira, J.C.; Santos, A.M. Effect of clay type on the properties of hybrid latexes of poly(vinyl acetate) and montmorillonite prepared via surfactant free emulsion polymerization. *Polym. Bull.* **2019**, *76*, 6305-6325, https://doi.org/10.1007/s00289-019-02708-z.
46. Batistella, M.; Otazaghine, B.; Sonnier, R.; Caro-Bretelle, A.-S.; Petter, C.; Lopez-Cuesta, J.-M. Fire retardancy of ethylene vinyl acetate/ultrafine kaolinite composites. *Polym. Degrad. Stab.* **2014**, *100*, 54-62, https://doi.org/10.1016/j.polymdegradstab.2013.12.026.
47. Sahoo, B.P.; Naskar, K.; Tripathy, D.K. Conductive carbon black-filled ethylene acrylic elastomer vulcanizates: physico-mechanical, thermal, and electrical properties. *J. Mater. Sci.* **2012**, *47*, 2421-2433, https://doi.org/10.1007/s10853-011-6065-8.
48. Manoharan, P.; Naskar, K. Plant Based Poly-functional Hindered Phenol Derivative as an Alternative for Silane in *Cis*-Polyisoprene and its Functionalized Derivative Systems Containing Nano-sized Particulates. *J. Polym. Environ.* **2018**, *26*, 1355-1370, https://doi.org/10.1007/s10924-017-1036-z.
49. Meneghetti, G.; Ricotta, M.; Lucchetta, G.; Carmignato, S. An hysteresis energy-based synthesis of fully reversed axial fatigue behaviour of different polypropylene composites. *Compos. B: Eng.* **2014**, *65*, 17-25, https://doi.org/10.1016/j.compositesb.2014.01.027.
50. Ge, S.; Li, M.; Ji, N.; Liu, J.; Mul, H.; Xiong, L.; Sun, Q. Preparation of a Strong Gelatin−Short Linear Glucan Nanocomposite Hydrogel by an in Situ Self-Assembly Process. *J. Agric. Food Chem.* **2018**, *66*, 117-186, https://doi.org/10.1021/acs.jafc.7b04684.
51. Datta, S.; Naskar, K.; Bhardwaj, Y.K.; Sabharwal, S. A study on dynamic rheological characterisation of electron beam crosslinked high vinyl styrene butadiene styrene block copolymer. *Polym. Bull.* **2011**, *66*, 637-647, https://doi.org/10.1007/s00289-010-0359-x.
52. Shibulal, G.S.; Naskar, K. RFL coated aramid short fiber reinforced thermoplastic elastomer: Mechanical, rheological and morphological characteristics. *J. Polym. Res.* **2011**, *18*, 2295-2306, https://doi.org/10.1007/s10965-011-9643-1.
53. Salimi, A.; Mirabedini, S.M.; Atai, M.; Mohseni, M. Oxidized Polypropylene Wax in Polypropylene Nanocomposites: A Comparative Study on Clay Intercalation. *Iran. Polym. J.* **2011**, *20*, 377-387.
54. Jena, D.P.; Anwar, S.; Parida, R.K.; Parida, B.N.; Nayak, N.C. Structural, thermal and dielectric behavior of two-dimensional layered $Ti_3C_2T_x$(MXene) filled ethylene–vinyl acetate (EVA) nanocomposites. *J. Mater. Sci. Mater. Electron.* **2021**, *32*, 8081-8091, https://doi.org/10.1007/s10854-021-05531-3.